

BEAM DYNAMICS, PERFORMANCE, AND TOLERANCES FOR PULSED CRAB CAVITIES AT THE ADVANCED PHOTON SOURCE FOR SHORT X-RAY PULSE GENERATION*

M. Borland[†], L. Emery, V. Sajaev, Argonne National Laboratory

Abstract

The Advanced Photon Source (APS) has decided to implement a system [1] using pulsed crab cavities to produce short x-ray pulses using Zholents' [2] scheme. This paper describes beam dynamics issues related to implementation of this scheme with one-sector separation between the cavities. Modeling of the cavity is used to demonstrate that the deflection will be independent of transverse position in the cavity but that there is a position offset for undeflected particles. Configuration and parameter choices to optimize performance are discussed. Finally, tolerances are discussed and determined based on tracking simulations.

INTRODUCTION

A significant segment of the storage ring light source user community is interested in time-resolved experiments. In many cases, the time resolution of interest is well below the typical 100-ps FWHM bunch durations available from storage rings at high current. However, providing high-intensity short pulses from a storage ring is problematical. Zholents' transverse chirping scheme [2] promises a reduction in pulse duration of two orders of magnitude with intensity that is 1% or more of normal. In this scheme, a transverse deflecting cavity is used to impose a quasilinear correlation between vertical momentum and arrival time. If an undulator is placed immediately following the cavity, or at a downstream location with $n\pi$ difference in vertical phase advance, then the photons from the undulator will have an angle-time correlation. This correlation can be used to perform time-slicing or, using suitable x-ray optics, time-compression. A second cavity at a downstream location with $n\pi$ difference in vertical phase advance is required in order to remove the chirp from the electron beam.

CAVITY PROPERTIES FOR MODELING

A 2D model of the actual cavity is sufficient to describe the effect of the main deflecting mode. In a cavity with open beam pipes, the main deflecting mode is a mixture of TM and TE modes. Particles will be deflected by both the E-field and the B-field. Figure 1 shows the field amplitudes (from an URMEL [3] calculation) and their special integrals for particle trajectories passing through the 3-cell cavity. In this cavity application the reference direction is the

y-axis, so E_r is E_y and H_ϕ is pointing in the $-x$ direction along the y-axis. Including time factors $\exp(i\omega t + \psi)$ and $\exp(i\omega t + \pi/2 + \psi)$, where ω is the oscillation frequency, for the E- and H-field amplitudes, respectively, the transverse momentum imparted can be calculated for arbitrary phase ψ , with the particle at the center of cavity at $t = 0$. For a centroid deflection, the cavity phase ψ is $\pi/2$, and the deflection is $\int E_r \sin(\omega z/c) ds - Z_0 \int H_\phi \cos(\omega z/c) ds$. For the chirp operation, the cavity phase ψ is 0, and the deflection is $\int E_r \cos(\omega z/c) ds - Z_0 \int H_\phi \sin(\omega z/c) ds$, i.e., zero. For a general phase, we sum the above results with weights $\cos \psi$ and $\sin \psi$, respectively.

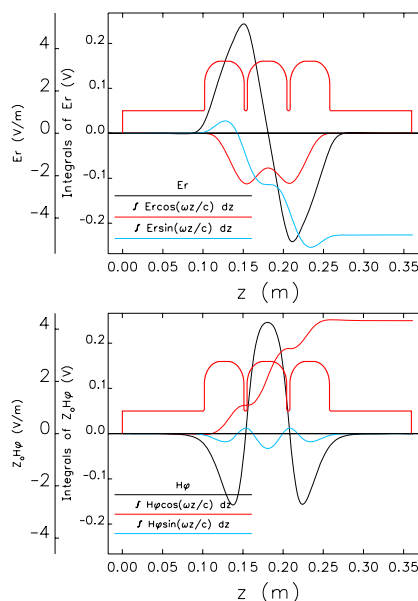


Figure 1: Field amplitudes $E_r(z)$ and $H_\phi(z)$ and their integrals through a 3-cell cavity with arbitrary normalization.

These integrals are a function of the radius of the trajectory, but the sum of the E- and H-field contributions is constant. This is shown in Figure 2 for a cavity phase of $\psi = \pi/2$, but is valid for all phases.

Previous beam dynamics studies [4] for the crab cavity scheme used a pure TM110-mode deflection (i.e., cavity with no open beam pipes), which has a natural dependence on radius. Eventual realization that the cavity mode was not a pure TM mode and that the deflection was independent of radius removed significant aberration terms in the particle tracking. Simulation of physical deflecting cavities in elegant [5] should use the RFDF element, which has constant deflection as a function of transverse coordinates,

* Work supported by the U.S. Department of Energy, Office of Science, Basic Energy Sciences, under Contract No. DE-AC02-06CH11357.

[†] borland@aps.anl.gov

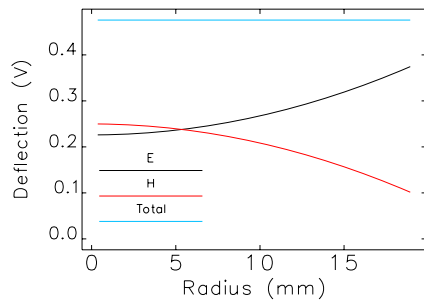


Figure 2: Deflection contributions and sum for the field levels in Figure 1

rather than the RFTM110 element.

The reference particle, having $\psi = 0$, receives no net deflection as seen from curves $\int E_r \cos(\omega z/c) ds$ and $\int H_\phi \sin(\omega z/c) ds$ in Figure 1. However, there are alternating deflections as the particle traverses the cavity, and hence a non-zero integral of the deflection. This may cause a net particle offset in the deflecting plane. One can see this mostly from the $\int E_r \cos(\omega z/c) ds$ curve. The beam offset depends on the variation of the fields in the end cells of the cavities, but is typically small (about $4 \mu\text{m}$ for the present application). This is included approximately in tracking studies by using non-zero-length RFDF elements.

CONFIGURATION AND PERFORMANCE

As discussed in [1], we originally planned to place three deflecting cavities in a single straight section, where they would act as a close chirp bump. However, space and performance issues make this unworkable. We plan to use two pairs of cavities separated by $n\pi$ phase advance in the vertical (deflecting) plane. More specifically, we separated the cavity pairs by one sector and thus serve a single APS undulator beamline. The cavities will be placed near the downstream end of both sectors. The vertical phase advanced per sector in the APS is normally 0.965π , which makes it fairly easy to adjust the lattice to get exactly π phase advance.

Since we intend to use a pair of 3-cell cavities at each location, we can null out the position offset of the ideal undeflected particle by adjusting the phases of the two cavities in each cavity pair in opposite directions.

This system will be operated only in the so-called “hybrid” mode. In this mode, we have a single 16-mA bunch on one side of the ring and 84 mA in 56 equally-populated bunches in a $0.5\text{-}\mu\text{s}$ -long train (with gaps) on the other side, leaving $1.59 \mu\text{s}$ on either side of the intense bunch. Only the intense bunch will be deliberately chirped. This bunch has an rms duration of about 70 ps due to potential well distortion, much longer than the 40-ps duration in the 24-bunch mode explored in [4]. This has implications both for single-particle dynamics and use of the chirped x-ray beam. It requires a chromaticity in each plane of $\partial\nu/\partial\delta = 11$, which makes achieving adequate dynamic and momentum aperture challenging.

As shown previously [4], the presence of sextupoles and uncorrected chromaticity between the cavities will result in emittance growth, potentially in both planes. This is worsened by the longer bunch, since it means more particles are kicked with large amplitudes. In [6], we showed that optimization of sextupoles can make the emittance growth manageable, provided one fixes the chromaticity between the cavities at zero and ensures that sextupole strength changes are not excessive. We performed this optimization procedure and additionally increased the spacing of the tunes by lowering the horizontal tune by 0.05, which decreases the degree to which the large vertical motion induced by the cavities gets coupled into the horizontal plane. Dynamic and momentum apertures were evaluated for the optimized sextupole values and found to be little different from those for the normal sextupole values.

Figure 3 shows the evolution of the vertical emittance following the beginning of 1-kHz cavity pulsing. These 10,000-turn results use 1000 particles tracked with Pelegant [7]. The equilibrium beam properties are taken as the average of the last 2000 turns. We start with an initial vertical emittance of 13 pm, corresponding to our operational minimum. For deflecting voltages of more than 4 MV/pair, the emittance growth becomes excessive, as the vertical emittance is larger than the nominal operating value of 25 pm. Figure 4 shows the vertical emittance vs deflecting voltage for nominal and optimized sextupoles. Horizontal emittance (not shown) is little affected.

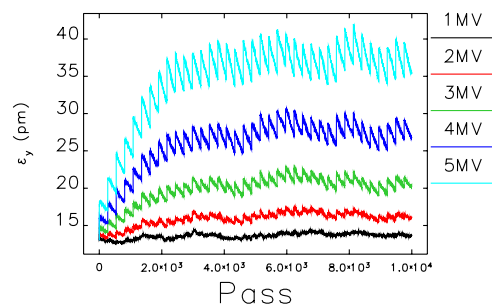


Figure 3: Evolution of vertical emittance for various total voltages on the first cavity pair.

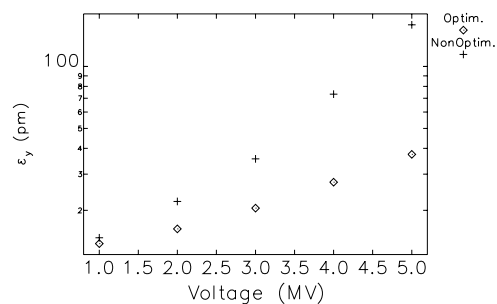


Figure 4: Trends in equilibrium vertical with and without sextupole optimization.

track one pass with 1 million particles to obtain the electron beam phase space at the center of the undulator. To compute the x-ray beam properties, we simulate the emission of a photon from each simulation electron using the single-electron photon distribution. This is obtained from the program *sddsurgent* [8] and is illustrated in Figure 5 for 10-keV radiation from a 2.4-m-long U33 undulator. Sampling and addition to the electron distribution is performed using *SDDS* tools [9]. We can then use drift and aperture elements in *elegant* to propagate and manipulate the resulting distribution. Figure 6 shows the results of a 30-m drift followed by slits. We see that there is little if any advantage in going beyond 4 MV, a result of the dramatic increase in vertical emittance above that level. X-ray pulse durations of 2 ps FWHM and transmission of 0.9% are predicted for a vertical slit half-height of 0.3 mm.

Off-axis second-harmonic radiation, seen as the large ring in Figure 5, increases the ultimate achievable pulse duration by $\sim 30\%$. More importantly, it creates satellite pulses on either side of the main pulse. These can be reduced in intensity using ± 0.75 mm horizontal slits [10], which are included in the above results.

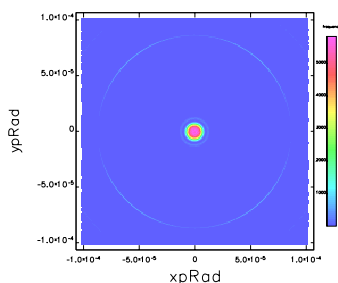


Figure 5: Single-electron angular radiation distribution for 10-keV radiation from a 2.4-m-long U33 undulator.

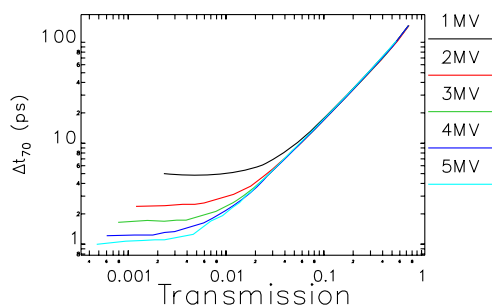


Figure 6: Duration of central 70% of x-ray pulse after vertical slits at 30 m, vs. transmission through slits.

TOLERANCES

Tolerances were previously investigated in detail for the cw case [4]. We anticipate that tolerances will be relaxed for the pulsed case because the rf voltage is lower and the

beam has time to damp between pulsing of the cavities. We looked at sensitivities by scanning various errors for the first cavity only. Figure 7 shows results for rf phase and voltage errors, which are the most worrisome. As discussed in [4], common-mode errors in voltage and phase have little or no impact on the beam. It is only differences in phase or voltage that produce significant emittance growth. Hence, when determining the error budget from these scans, we have six sources of error (three phases and three voltages), rather than eight, since one cavity acts as the phase and voltage reference for the others. We have, somewhat arbitrarily, decided that errors should increase the emittance by no more than 10% above the nominal equilibrium level of 27.5 μm . The effects shown in Figure 7 are accurately described by quadratic dependences on phase and voltage, respectively. Because the emittance only increases, the contributions add directly rather than in quadrature. Hence, to limit the emittance increase to 2.8 μm , we should require all six contributions to add no more than 1/6 of this value. These levels are shown on Figure 7 as horizontal lines, from which we determine that the phase tolerance is $\pm 0.07^\circ$ and the voltage tolerance is $\pm 0.12\%$.

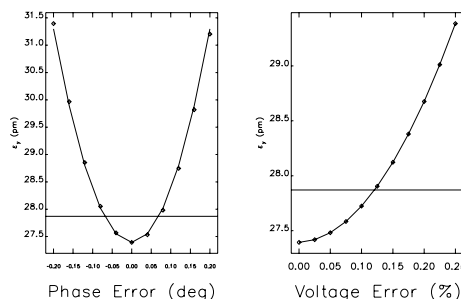


Figure 7: Effect of phase and voltage errors on the equilibrium emittance for 4-MV total deflection from the first two cavities.

REFERENCES

- [1] M. Borland *et al.*, "Planned Use of Pulsed Crab Cavities for Short X-ray Pulsed Generation at the Advanced Photon Source," these proceedings.
- [2] A. Zholents *et al.*, NIM A 425, 385 (1999).
- [3] T. Weiland, NIM 216, 329-348 (1983).
- [4] M. Borland, Phys. Rev. ST Accel. Beams 8, 074001 (2005).
- [5] M. Borland, Advanced Photon Source LS-287, September 2000.
- [6] M. Borland *et al.*, Proc. 2005 PAC, 3886-3888.
- [7] Y. Wang *et al.*, "Implementation and Performance of Parallelized *elegant*," these proceedings.
- [8] H. Shang, based on US by R. Dejus and URGENT by R. Walker.
- [9] R. Soliday *et al.*, Proc. 2003 PAC, 3473-3475.
- [10] V. Sajaev *et al.*, Proceedings of SRI2007 Conference, to be published.